Supporting Information

High loading accessible activity sites via designable 3D-printed metal architecture towards promoting electrocatalytic performance

Shuai Chang,‡[a,b] Xiaolei Huang,‡[c] Chun Yee Aaron Ong,[b] Liping Zhao,[d] Liqun Li,[a] Xuesen Wang,[c] Jun Ding[b]*

[a]*State Key Laboratory of Advanced Welding and Joining,*
Harbin Institute of Technology, Harbin, 15001, China.

[b]*Department of Materials Science and Engineering, Faculty of Engineering, National University of Singapore, 9 Engineering Drive 1, Singapore 117576, Singapore.*
E-mail: msedingj@nus.edu.sg

[c]*Department of Physics, Faculty of Science,*
National University of Singapore, 2 Science Drive 3, Singapore 117542, Singapore.

[d]*National Metrology Centre (NMC),*
*A*STAR, 1 Science Park Drive, Singapore 118221, Singapore.*

** Corresponding authors*

‡ These authors contributed equally to this work.

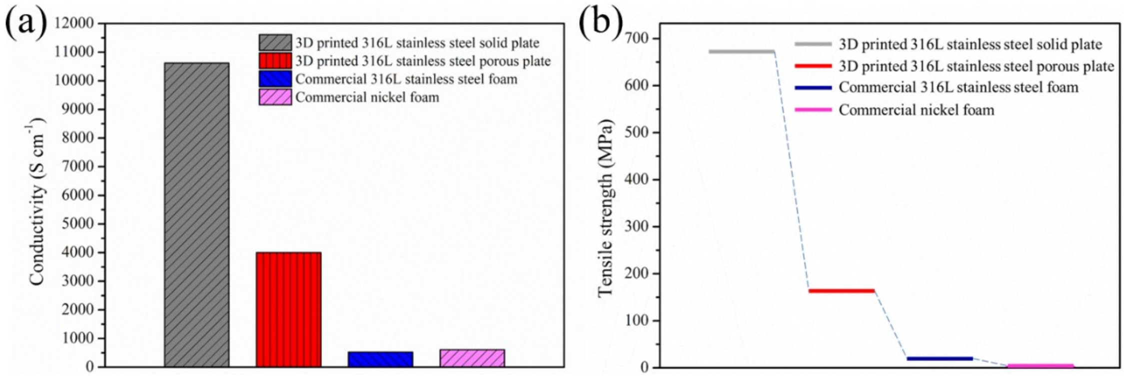

Figure S1. (a) Conductivity and (b) tensile strength of 3D printed 316L stainless steel solid plate, 3D printed 316L stainless steel porous plate, commercial 316L stainless steel foam, and commercial nickel foam.

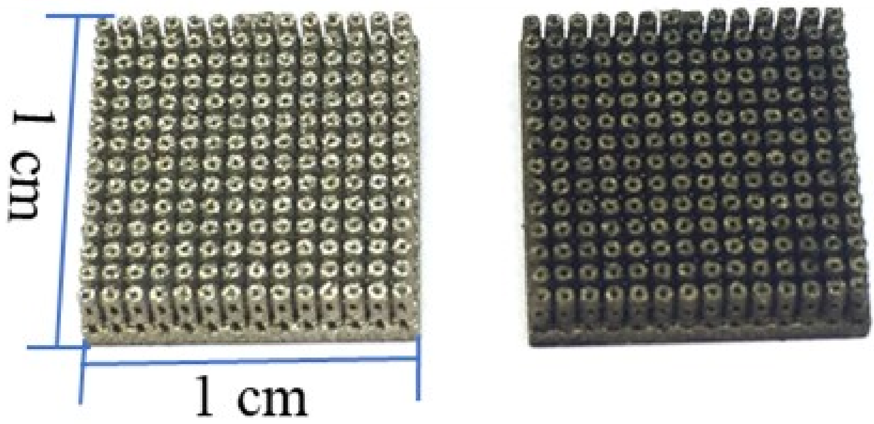

Figure S2. Photos of 3D printed electrocatalytic support (#6 support) before (left) and after (right) coating $NiCo_2S_4$ nanoneedles (#6N electrode).

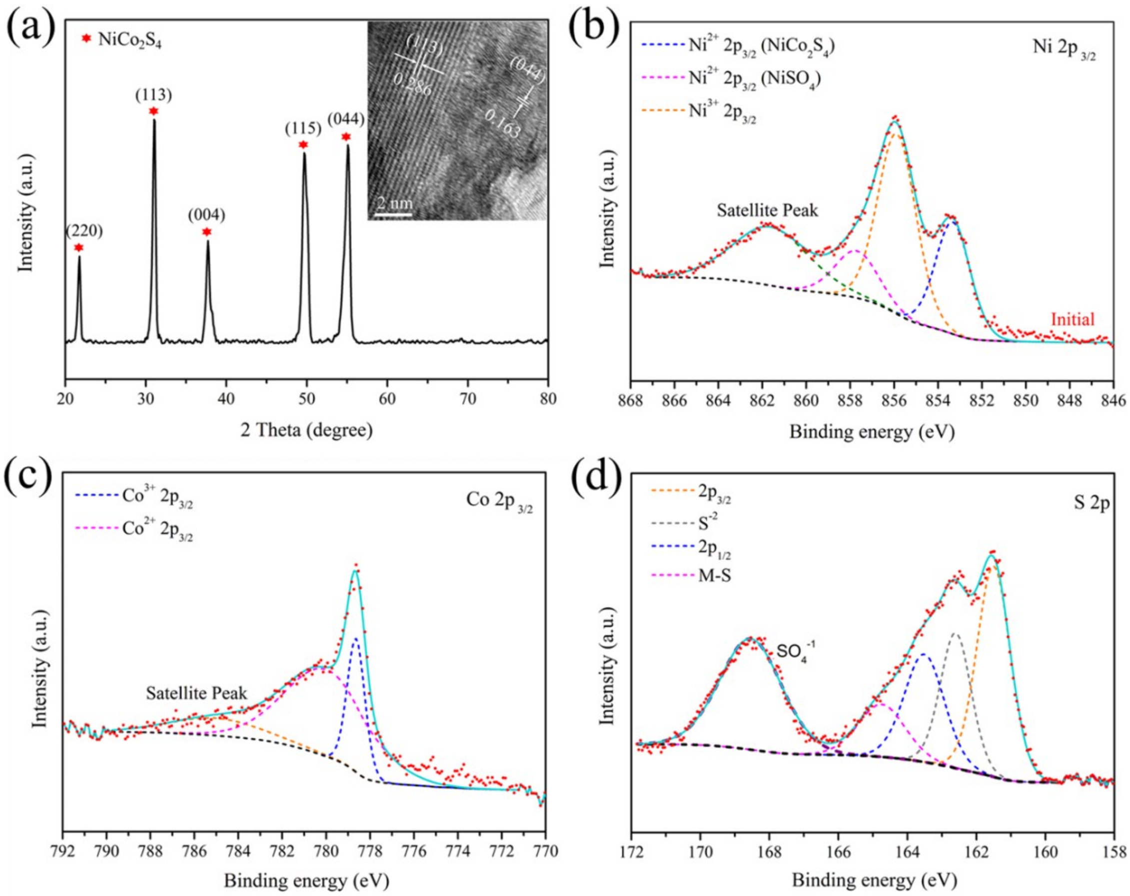

Figure S3. (a) XRD patterns of $NiCo_2S_4$ nanoneedles on #6N electrode. Inset: High-resolution TEM image of $NiCo_2S_4$ nanoneedles. (b) Ni 2p, (c) Co 2p and (d) S 2p XPS spectra for $NiCo_2S_4$ nanoneedles on #6N electrode.

XRD, TEM and XPS were used for the structural evaluation of $NiCo_2S_4$ nanoneedles. Crystalline $NiCo_2S_4$ phase was confirmed in our XRD examination (Figure S3a). $NiCo_2S_4$ nanoneedles were detached ultrasonically from the support for TEM examination. The measured lattice spacing between two fringes in high-resolution TEM (Figure S3a inset) were 0.286 nm and 0.163 nm, which is the diffraction of the (113) and (044) lattice planes, respectively, of the $NiCo_2S_4$ phase.[1,2] We used XPS to characterize the chemical valence states of the various elements in the $NiCo_2S_4$ nanoneedles structure. Figure S3b-S3d displays the typical fitted Ni 2p, Co 2p and S 2p XPS spectra of the $NiCo_2S_4$ nanoneedles. It can be found that the sample had a composition of Co^{2+}, Co^{3+}, Ni^{2+}, and Ni^{3+}cations, metal-S (M–S) bonds, and S^{2-} anions, which is consistent with that of reported $NiCo_2S_4$. [3,4] In summary, the $NiCo_2S_4$ catalyst was confirmed to be well-gown on the 3D printed support.

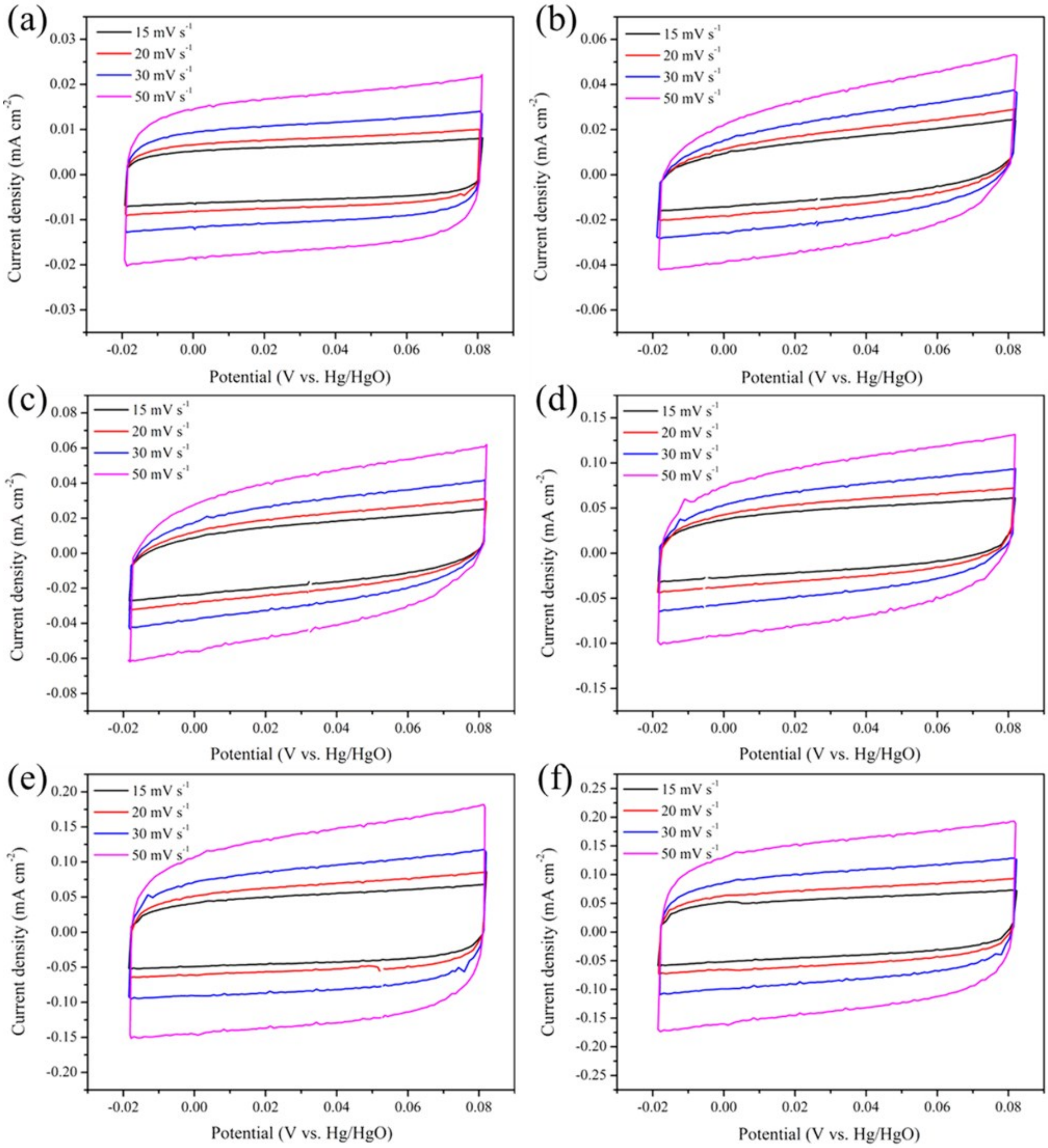

Figure S4. Cyclic voltammograms of 3D printed supports with various structures. (a) #1 support. (b) #2 support. (c) #3 support. (d) #4 support. (e) #5 support. (f) #6 support.

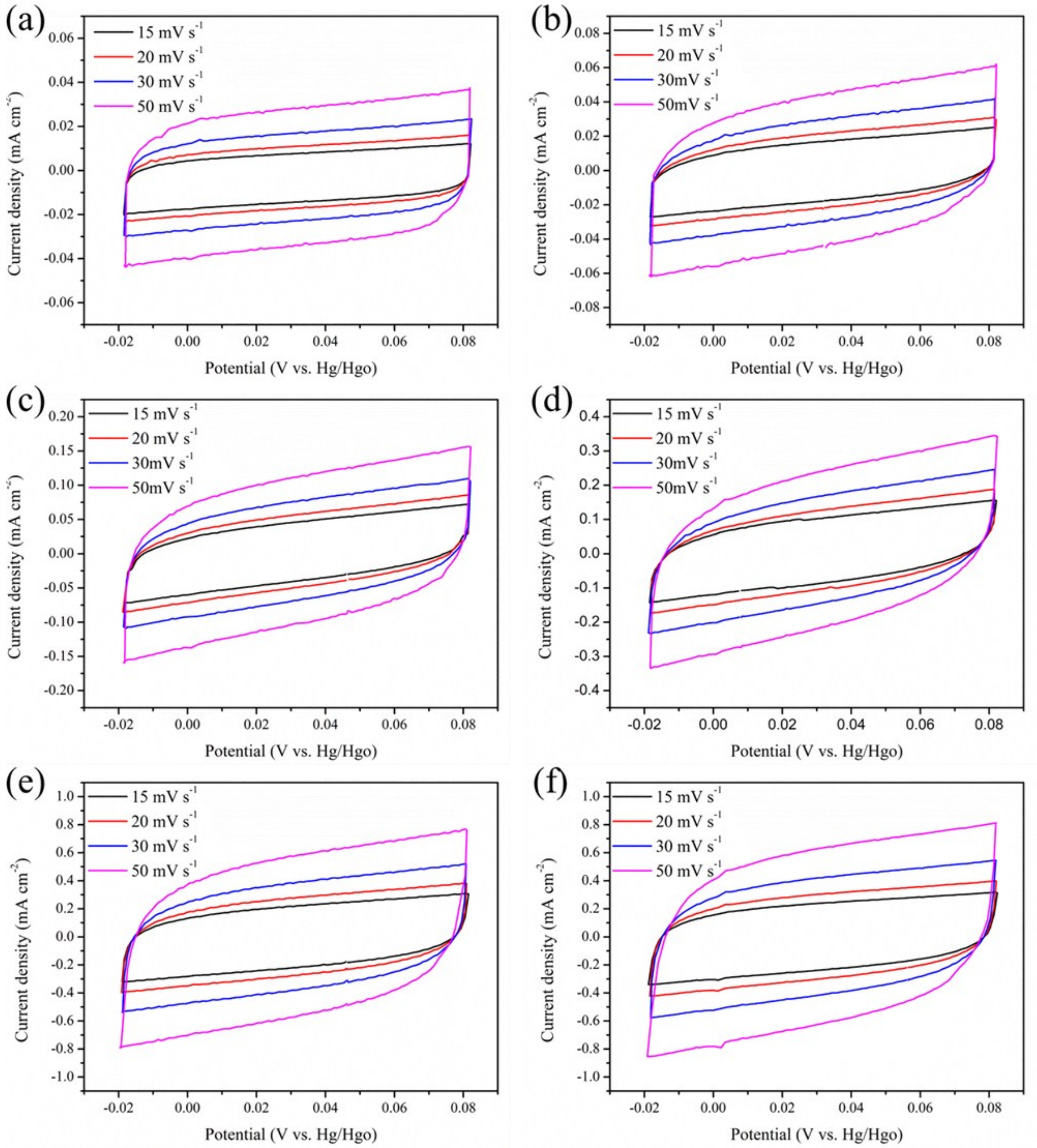

Figure S5. Cyclic voltammograms of 3D printed supports with in-situ growth of $NiCo_2S_4$ nanoneedles. (a) #1N electrode. (b) #2N electrode. (c) #3N electrode. (d) #4N electrode. (e) #5N electrode. (f) #6N electrode.

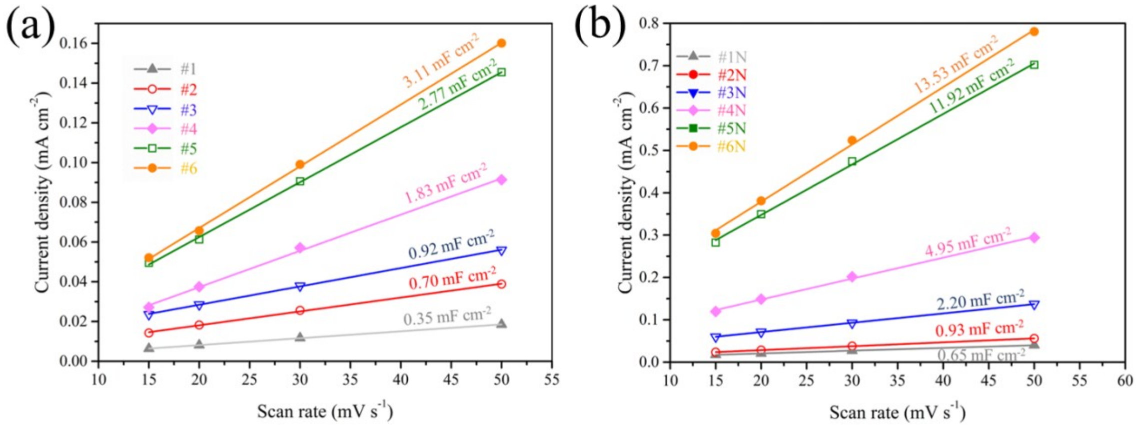

Figure S6. (a) Cathodic current measured at 0 V (vs. Hg/HgO) as a function of scan rate for 3D printed supports. (b) Cathodic current measured at 0 V (vs. Hg/HgO) as a function of scan rate for electrodes.

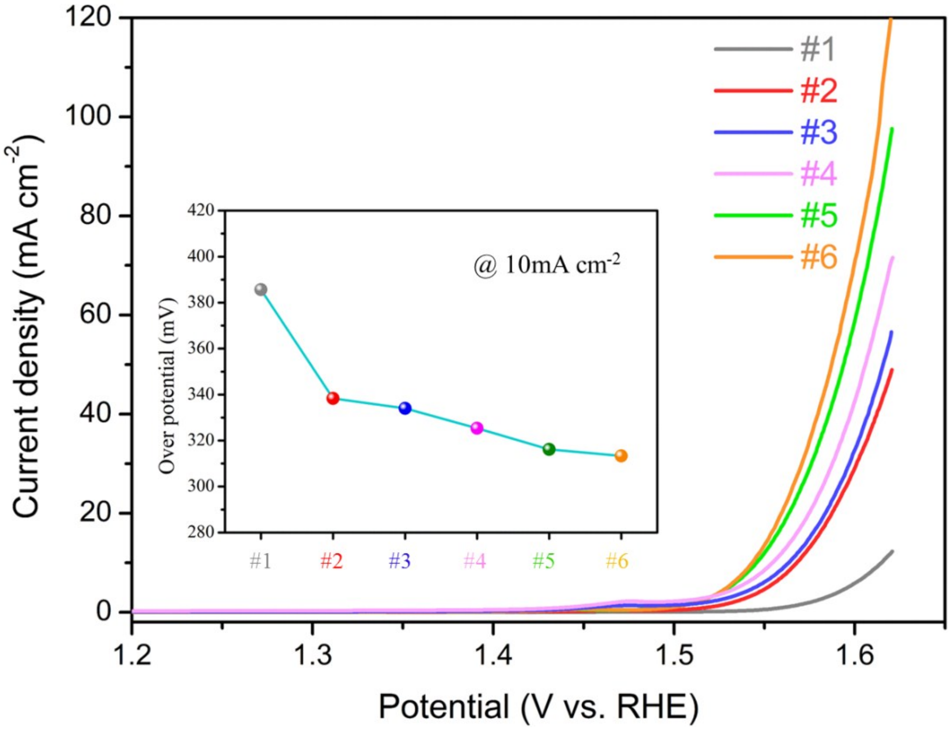

Figure S7. Polarization curves of 3D printed supports at a scan rate of 1 mV s^{-1}. Inset: Overpotential of 3D printed supports at a current density of 10 mA cm^{-2}.

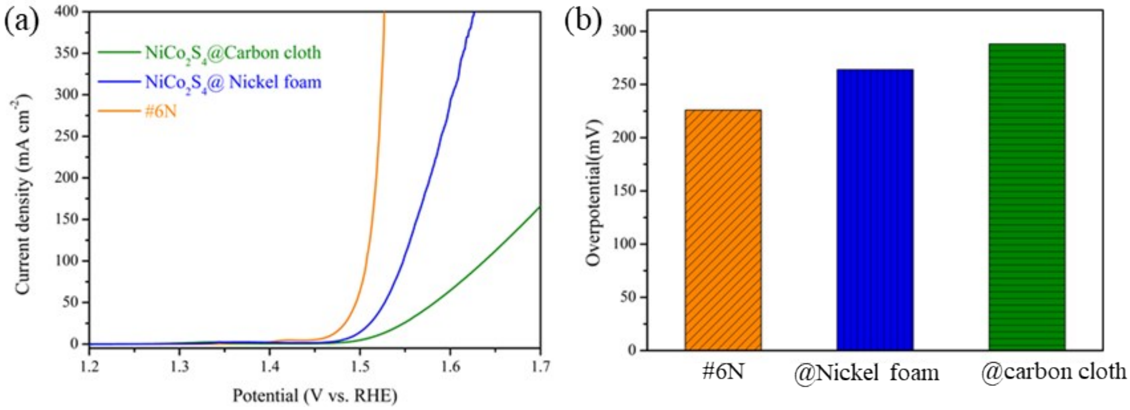

Figure S8. (a) Polarization curves of #6 N, $NiCo_2S_4$@Carbon cloth and $NiCO_2S_4$@Nickel foam electrodes at a scan rate of 1 mV s^{-1} with 85% iR compensation. (b) Overpotetnials of $NiCo_2S_4$ with various supports at a current density of 10 mA cm^{-2}.

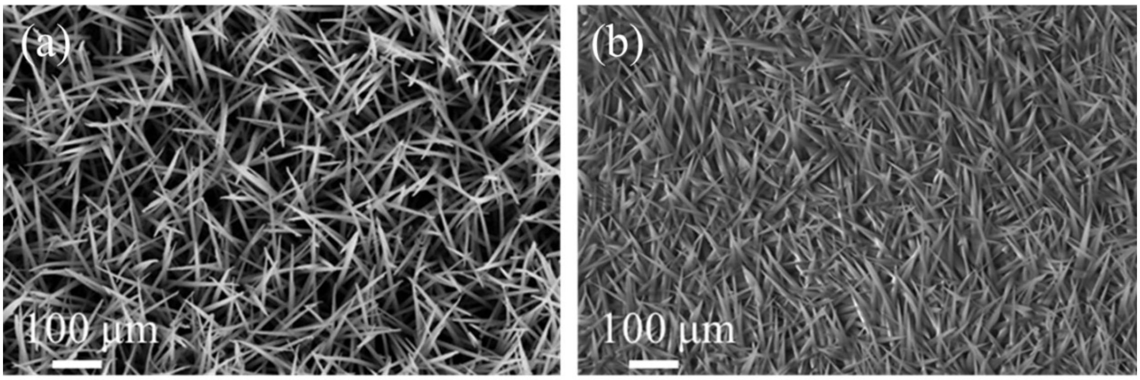

Figure S9. SEM images of $NiCo_2S_4$ catalyst coated on 3D printed support (#6N electrode). (a) Initial. (b) After 2000 LSV cycles.

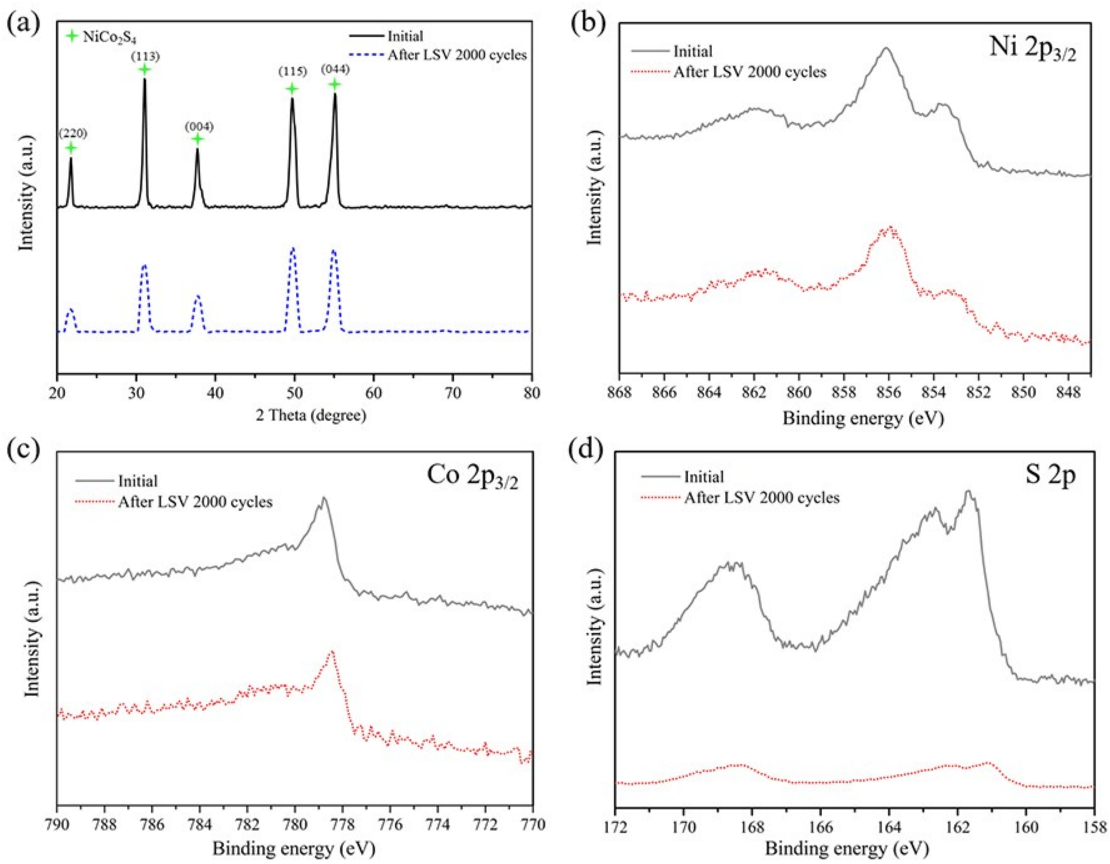

Figure S10. (a) XRD patterns of $NiCo_2S_4$ nanoneedles on #6N electrode. (b) Ni 2p, (c) Co 2p and (d) S 2p XPS spectra for $NiCo_2S_4$ nanoneedles on #6N electrode. Top: initial, down: after LSV 2000 cycles

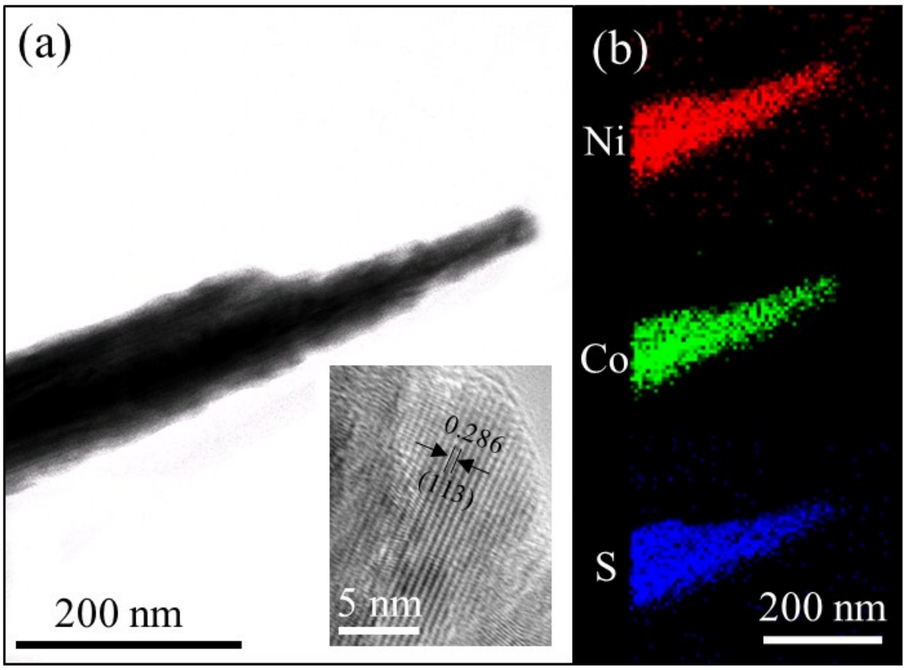

Figure S11. (a) TEM image of single $NiCo_2S_4$ nanoneedle after LSV 2000 cycles. Inset: High resolution TEM image. (b) Elemental mappings for Ni, Co and S.

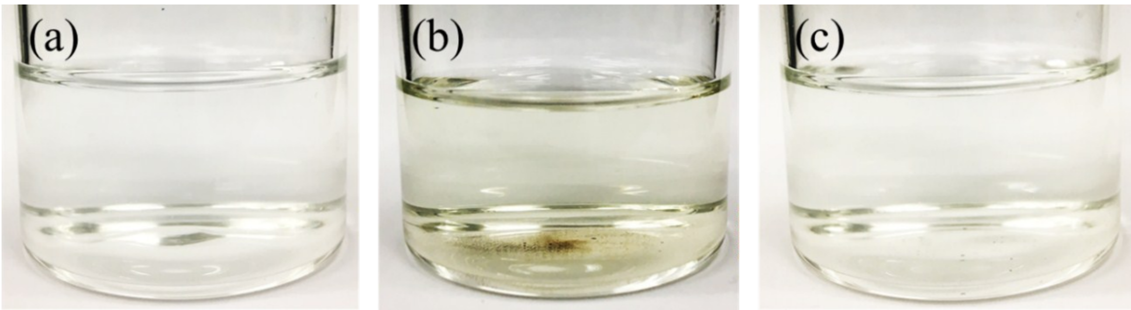

Figure S12. Photos of electrolyte (1M KOH) before and after chronopotentiometry test for 50 hours with a current density of 10 mA cm^{-2}. (a) Initial electrolyte (clear and colorless). (b) Electrolyte after chronopotentiometry test using as-printed #6 support. (b) Electrolyte after chronopotentiometry test using #6N electrode ($NiCo_2S_4$ catalyst coated on 3D printed support).

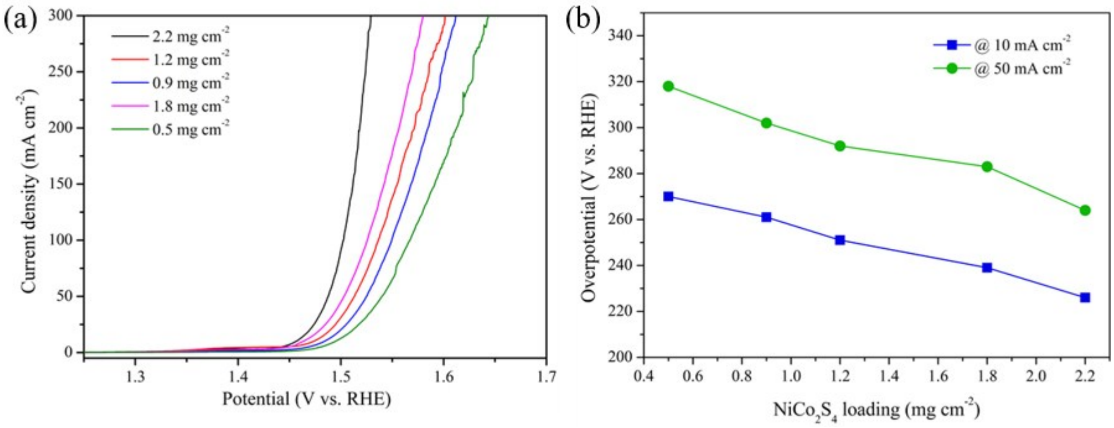

Figure S13. (a) Polarization curves of the optimized #6N electrode with loading various amount of $NiCo_2S_4$ catalyst at a scan rate of 1 mV s^{-1} with 85% iR compensation. (b) Corresponding overpotentials as a function of loading of $NiCo_2S_4$ catalyst.

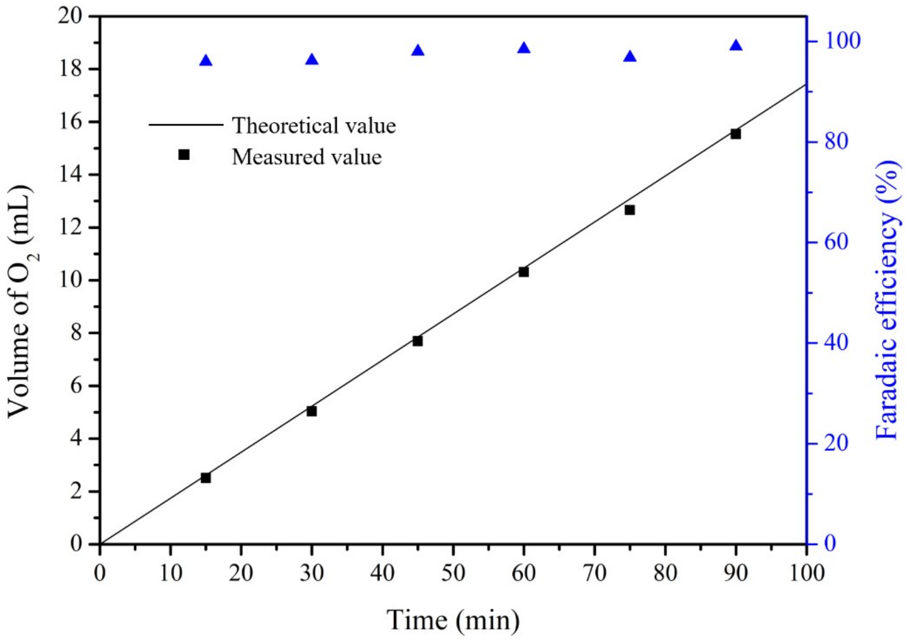

Figure S14. Electrocatalytic efficiency of O_2 production over #6N electrode at a current density of ca. 50 mA cm^{-2}, measured for 90 minutes.

Table S1. Comparison of OER performances of representative $NiCo_2S_4$ based electrocatalysts with different supports in 1M KOH.

Support	Overpotential (mV) @10 mA cm^{-2}	Overpotential (mV) @ 50 mA cm^{-2}	Overpotential (mV) @ 100 mA cm^{-2}	Tafel slope mV dec^{-1}	Dura-bility h	Ref.
#6	226	264	277	38.7	50	This work
#1	308	-	-	45.0	-	This work
NiCo coated nickel foam	-	330	340*	73.2	-	[5]
Nickel foam	320*	372	420*	71.5	-	[5]
Nickel foam	310*	381*	409	91.0	-	[6]
Nickel foam	-	300*	319	53.3	-	[3]
Graphdiyne foam	308*	328	338	47.0	-	[7]
Carbon cloth	323*	376	402	76.0	-	[7]
Nickel foam	260	345*	384*	40.1	50	[1]
Carbon cloth	309*	322*	340	89.0	-	[2]
Reduced graphene oxide	467	-	-	-	-	[8]
Glassy carbon	337	-	-	64.0	30	[9]

(*) The overpotetnial was estimated from the corresponding polarization curves.

Reference:

[1] A. Sivanantham, P. Ganesan and S. Shanmugam, *Advanced Functional Materials*, 2016, **26**, 4661-4672.

[2] D. Liu, Q. Lu, Y. Luo, X. Sun and A. M. Asiri, *Nanoscale*, 2015, **7**, 15122-15126.

[3] J. Yu, C. Lv, L. Zhao, L. Zhang, Z. Wang and Q. Liu, *Advanced Materials Interfaces*, 2018, **5**, 1701396.

[4] X. Wu, S. Li, B. Wang, J. Liu and M. Yu, *Phys Chem Chem Phys*, 2017, **19**, 11554-11562.

[5] Y. Ning, D. Ma, Y. Shen, F. Wang and X. Zhang, *Electrochimica Acta*, 2018, **265**, 19-31.

[6] X. Yin, G. Sun, L. Wang, L. Bai, L. Su, Y. Wang, Q. Du and G. Shao, *International Journal of Hydrogen Energy*, 2017, **42**, 25267-25276.

[7] Y. Xue, Z. Zuo, Y. Li, H. Liu and Y. Li, *Small*, 2017, **13**.

[8] Q. Liu, J. Jin and J. Zhang, *ACS Appl Mater Interfaces*, 2013, **5**, 5002-5008.

[9] J. Jiang, C. Yan, X. Zhao, H. Luo, Z. Xue and T. Mu, *Green Chemistry*, 2017, **19**, 3023-3031.